Research Article | Vol. 27, No. 21 / 14 October 2019 / Optics Express 30597
Optics EXPRESS

All-reflective electronic viewfinder enabled by freeform optics

AARON BAUER,[1,*] MATTHIAS PESCH,[2] JULIUS MUSCHAWECK,[2,3] FLORIAN LEUPELT,[2] AND JANNICK P. ROLLAND[1]

[1]The Institute of Optics, University of Rochester, 275 Hutchison Road, Rochester, NY 14627, USA
[2]Arnold & Richter Cine Technik GmbH & Co Betriebs KG, Türkenstraße 89, D-80799 München, Germany
[3]JMO GmbH, Zugspitzstr. 66, D-82131 Gauting, Germany
[*]aaron.bauer@rochester.edu

Abstract: Refractive eyepiece design forms are often limited by chromatic aberrations and require a mix of glass types to achieve sufficient correction, thus they are not conducive to manufacture in volume. Reflective surfaces are inherently achromatic and can be produced in volume, but rotationally symmetric reflective surfaces are either used with lossy obscurations or are incapable of correcting rotationally variant aberrations when used in an unobscured form. Freeform optics enable unobscured reflective design forms with excellent image quality. Here, we document the design, fabrication, and assembly of an all-reflective high-end electronic viewfinder that shows the applicability of freeform surfaces to eyepiece design forms.

1. Introduction

In today's professional digital photography and videography, there has been a transition from optical viewfinders, where the scene is directly viewed by the operator, to electronic viewfinders, where the scene is first captured by the digital camera, and subsequently presented on a small electronic display that is viewed through an eyepiece. As the resolution of imaging sensors and displays increases over time, viewfinder optical performance must also evolve to enable camera operators to take full advantage of resolution progress. Similarly, decreasing the size and weight of the viewfinder makes the task of carrying and transporting the camera less stressful on the operator.

In addition to having superb aberration correction over a large field-of-view (FOV) and eyebox, an electronic viewfinder for a high-end professional camera must be corrected for distortion and have high color uniformity across the FOV. The color uniformity requirement translates into a tight specification on the chief-ray angle (telecentricity) at the display within the viewfinder due to color shifting of the miniature display at different angles. Combined, these specifications define a challenging optical design problem.

The design form of an electronic viewfinder is essentially an eyepiece, where the aperture stop (entrance pupil/eyebox for visual instruments) is located external to the system and coincident with the operator's eye when used. The external aperture stop causes a large degree of asymmetry relative to the aperture stop, which is an indication that aberrations with odd parity, such as coma and distortion, will tend to be large. Additionally, as most conventional eyepieces are refractive, they suffer from significant lateral color, which is magnification as a function of wavelength. Correction of lateral color is a major hurdle which must be overcome to design a viewfinder system that meets the requirements for a high-end camera. For refractive systems, this is achieved by using a variety of glass types with different refractive indices and Abbe numbers [1]. This method can sometimes include using glasses with atypical dispersion, which can be expensive and difficult to grind and polish into lenses, thus are not conducive for large volume production.

An alternative solution to the problem of lateral color correction is to forego using lenses altogether and to use solely reflective optics, which are inherently achromatic and can be molded

#374523 https://doi.org/10.1364/OE.27.030597
Journal © 2019 Received 6 Aug 2019; revised 25 Sep 2019; accepted 30 Sep 2019; published 8 Oct 2019

Optics EXPRESS

and mirror coated. However, using reflective optics in an eyepiece form is an issue due to obscurations. One way to fully unobscure the FOV is to tilt the reflective surfaces, but this method is accompanied by significant blurring aberrations whose field dependences are no longer rotationally invariant [2–4]. Rotationally variant aberrations are a problem that freeform surfaces are uniquely suited to solve. By designing an eyepiece with freeform reflective surfaces, lateral color is nonexistent, the system can be fully unobscured, and the aberrations can be corrected to yield a high-end viewfinder system. In this work, we describe the comprehensive design, fabrication and user testing of an all-reflective, freeform, five mirror high-end (i.e. professional video camera) electronic viewfinder.

2. Design specifications and approach

The design of the viewfinder system is approached as an eyepiece design, except where an eyepiece would be coupled to an intermediate image, the viewfinder is coupled with an electronic display. The display in this case is an organic light emitting diode (OLED) microdisplay. OLED microdisplays are self-emitting, so no auxiliary illumination optics are required, which simplifies the system design. However, OLED microdisplays can suffer from color non-uniformity over the full viewing angle, which necessitates a strict image telecentricity requirement of $<2^\circ$ angle of incidence of the chief rays on the image plane. Because most camera operators prefer to work without eyeglasses, the viewfinder must also be corrected over a range of focusability from at least -5 diopters to $+5$ diopters, where the majority of the population falls. Additionally, 25 mm of free space between the eyebox and the closest mechanical surface of the viewfinder assembly is required for comfort. Full design specifications can be found in Table 1. These specifications are highly competitive with currently marketed high-end electronic viewfinders.

Table 1. Design specifications.

Parameter	Unit	Specification
Image size when viewed @ 10 ft.	inch	72 (diag.)
Eyebox diameter	mm	12
Eye clearance	mm	25
Focus adjustment	diopter	± 5
Image distortion	percent	< 2
Display-space telecentricity	degree	< 2
MTF @ Nyquist freq. of display	percent	> 25
Microdisplay resolution	pixel	1920×1080
Pixel pitch	μm	8.1

Given the FOV and the size of the OLED, the focal length, f, can be calculated using $h = f\tan(\theta)$, where h is the semi-diagonal of the microdisplay and θ is the diagonal half FOV. It was shown in [5] that a two-freeform-mirror solution can be implemented, however with the more stringent requirements of this system, the distortion, telecentricity, FOV, and image quality specifications cannot be simultaneously met with two mirrors. Adding a third freeform mirror allows additional degrees of freedom, but also increases the total optical path that must be traveled by the light. Maintaining a geometry that is completely unobscured with three mirrors comprises more optical path than can be feasibly traversed by the light before coming to a focus for the given focal length. Therefore, when considering solutions of 3+ mirrors, reimaging type systems are considered. As an additional benefit of a reimaged system, the external aperture stop can be imaged to a plane coincident with an optical surface, which allows field-constant aberrations to be more readily corrected. Three mirrors allowed sufficient image quality and distortion correction but resulted in a physically large system and insufficient telecentricity correction. Adding a fourth freeform

Optics EXPRESS

mirror allowed the system to be folded into a tighter volume, but still did not provide sufficient simultaneous distortion and telecentricity control. A fifth, near flat freeform mirror, was added near the OLED plane to give precise control over the chief rays (i.e. distortion, telecentricity), while allowing further volume reduction.

All design requirements were met in a five freeform mirror geometry that fills up a space of around 200 cm^3 and is shown in Fig. 1. The design and optimization method that was utilized expands on that described in [6], and similarly, uses Zernike polynomials to describe the freeform shapes. The general procedure may be summarized as follows. First, determine the limiting aberrations using aberration full-field displays. Then, consult the aberration theory of freeform surfaces [4] to understand which shape of freeform is necessary to correct those aberrations. Finally, using the optimization routines in commercial raytrace software, determine how much of that shape is necessary. This process continues until the performance specification is met or further improvement cannot be achieved.

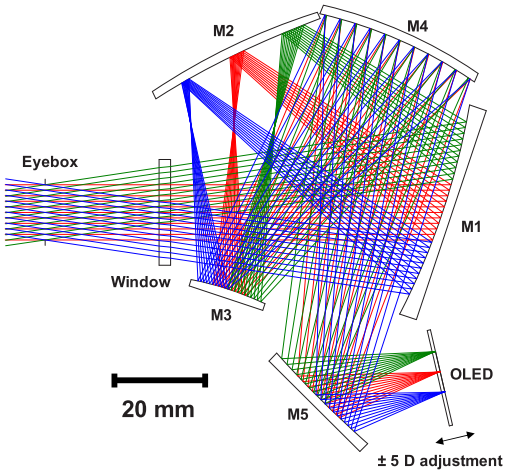

Fig. 1. Optical layout of the final 5-mirror viewfinder design.

Diopter adjustment was implemented by allowing the OLED to travel axially resulting in various levels of convergence at the eyebox. Image quality is evaluated over 4 mm subpupils that roam the full 12 mm eyebox. The MTF for the worst performing 4 mm subpupil at the + 5, 0, and −5 diopter positions is shown in Fig. 2, with vertical bars showing the MTF design goals.

The specific folding geometry of the 5-mirror system was determined by considering the aberrations generated from the tilting of the mirrors that then require correction with freeform surfaces and by optimizing the volume required for the five mirrors. It was shown in [6] that certain aberration combinations can be more efficiently corrected using freeform surfaces, so we look for those geometries. The optimal tilts of the first two mirrors were then chosen in accordance with Bauer et al. [5], which showed the best orientation for two positive mirrors. The third and fourth mirrors are negative and positive, respectively, and their tilts were chosen to be in the same direction as in the classical three-mirror-anastigmat form [7] when referenced from the tilted secondary mirror and when the first two mirrors are considered as a single positive group. The fifth mirror is essentially a flat freeform targeted at correcting distortion and does not significantly affect the other aberrations. Its folding direction was chosen to minimize the system volume.

Optics EXPRESS

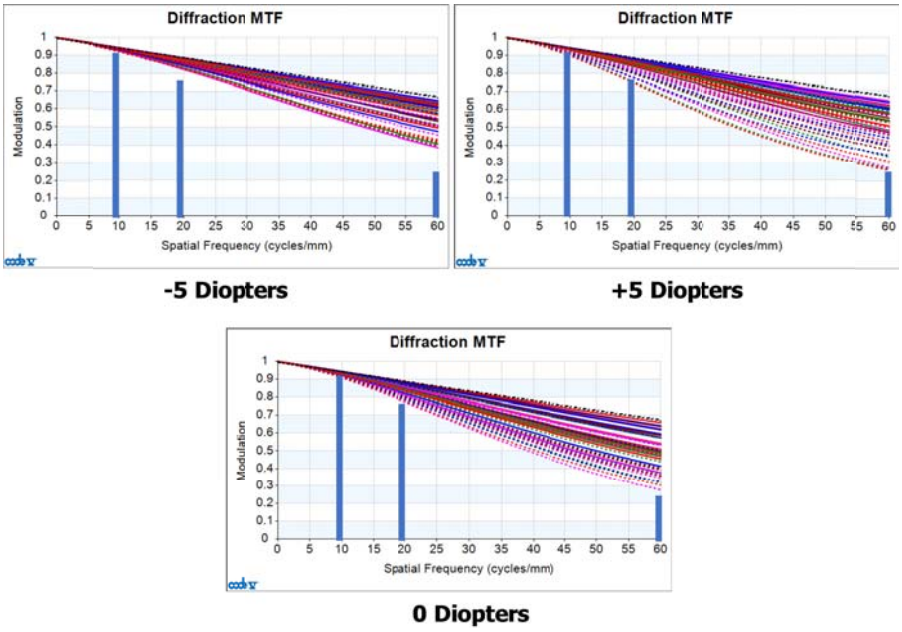

Fig. 2. MTF plots for the final nominal design evaluated over the worst 4 mm subpupil within the full 12 mm eyebox and shown for the + 5, −5, and 0 diopter focus positions. The vertical blue bars indicate the MTF goals for the nominal design.

3. Sensitivity and stray light analysis of final design

With the nominal design of the viewfinder complete, we must determine if the system can maintain performance after manufacturing tolerances are included in the analysis, which is a critical aspect of assessing a freeform design. Using ultra-precision machining, tight tolerances can be achieved for the placement of the optics. The applied tolerances are shown in Table 2. For the + 5, 0, and −5 diopter focus positions, a Monte-Carlo tolerance analysis was performed. Each parameter was perturbed with a random value within the tolerance range for each of the movable variables. After all perturbations, the focus was adjusted and the MTF of the system was evaluated over 4 mm subpupils that sample the full 12 mm eyebox. This procedure was repeated 2000 times and the results for the worst-performing subpupil are reported in Table 3. The MTF values over the FOV after tolerances have been applied meet the specification goals. The MTF drop after tolerances was <17%, which is acceptable and suggests that an even larger diopter correction range is therefore quite possible, although not investigated further here.

Table 2. Assembly and figure tolerances. Units of waves are measured at $\lambda = 587$ nm.

Parameter	Unit	Tolerance
Surface Tip/Tilt (M1,M2,M4)	minutes	± 1
Surface Tip/Tilt (M3,M5)	minutes	± 3
Surface clocking	minutes	± 1
X/Y/Z placement	μm	± 25
Surface astigmatism	waves	± 0.5
Surface coma	waves	± 0.5
Surface spherical ab.	waves	± 0.5

Optics EXPRESS

Table 3. MTF results of Monte Carlo analysis using the tolerances listed in Table 1 evaluated over the worst performing subpupil for the 0° and 90° azimuths at 40 cyc/mm.

	−5 Diopter		0 Diopter		+5 Diopter	
	0°	90°	0°	90°	0°	90°
Min % MTF	50	47	51	49	45	46
Avg % MTF	66	63	65	69	64	58
Max % MTF Drop	17	10	12	8	16	7
Avg % MTF Drop	7	2	6	5	8	5

Another aspect of a high-end camera viewfinder that must be satisfied is stray light suppression, which influences how a scene looks to the operator and, therefore, how the operator records it. To evaluate the main sources of stray light within the viewfinder system, a solid model of the system was generated and loaded into a non-sequential ray tracing software package. Since the operator's eye and face will block off the only opening to the inside of the viewfinder, the only light source modeled was the OLED microdisplay. The housing of the viewfinder was not modeled, though it is assumed that the non-optical surfaces inside of the viewfinder will be coated with a highly absorptive paint to minimize the scatter. The OLED was modeled as a rectangular source with Lambertian emittance and the reflective sources were modeled as 100% reflective. Six paths from the OLED to the eyebox were identified and are shown in Fig. 3, including the intended path. Three baffles were used to block the five unintended paths from being seen by the operator. The baffles can be seen in Fig. 3.

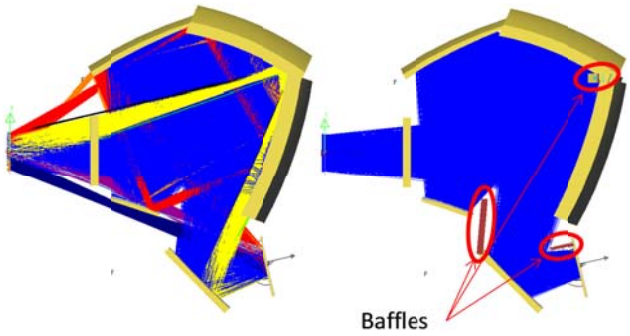

Fig. 3. (left) The paths from the OLED to the eyebox are shown, where the royal blue rays take the intended path and all other colored rays take a different path and are, therefore, considered stray light. (right) With the addition of 3 baffles to the design, all of the stray light can be blocked without vignetting the FOV. The mirrors were modeled as 100% reflective and all other surfaces were modeled as 100% absorptive.

4. Fabrication, assembly, and testing

For the fabrication of the mirrors, diamond machining was chosen. As a baseline, the rough surface structures of the mirrors were milled into a steel substrate and then the substrate surface was nickel-plated. By using the diamond machining process, the final shape was turned into the nickel layer. To reduce the amplitude of mid-spatial frequency tool marks that occur in the diamond machining process, the surfaces were gently hand-polished to their final roughness. While the use of nickel allows for a high surface quality [8], its reflective properties in the visible range are unsuitable for the viewfinder application, leading to significant losses for a five-mirror system. To maximize the light throughput of the system, the surfaces were coated with a protected

Optics EXPRESS

silver coating in an ion-plating process, resulting in a single-surface reflectivity of >98% in the visible range. A similar approach was taken with diamond machining of copper and coating with gold for a 3-mirror freeform infrared imager [9,10]. A visual inspection of the final surfaces shows that residual roughness patterns can be observed, especially in the off-center areas of the mirrors (see Fig. 4). No surface is close to the intermediate image, and therefore it is expected that while these roughness patterns may cause an overall loss of contrast, they will not be visibly apparent in actual operation.

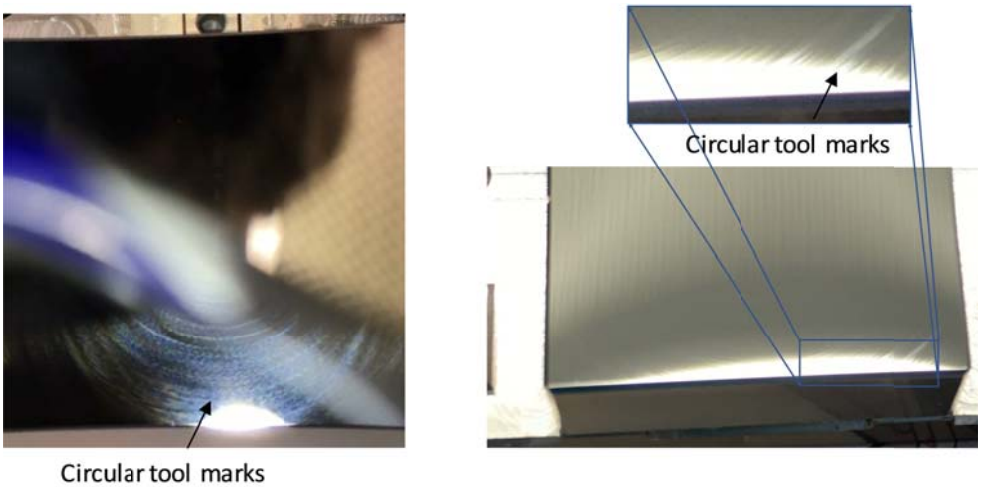

Fig. 4. Examples of the residual surface roughness on a freeform mirror due to the diamond machining.

Given the need for tight tip/tilt tolerances on the mirrors as found in the tolerance analysis, we decided for a mounting concept that ensures high precision placement of the optical surfaces without any adjustment mechanisms after mounting. A monoblock structure was designed and fabricated using a high-precision electrical discharge machining wire-cutting process, as shown in Fig. 5. The wire-cutting process results in mechanical tolerances of less than 10 µm, ensuring precise positioning of all mounting planes. All mirror substrates were mounted onto high precision mount plates with ± 10 µm tolerance. The mount plates were then doweled onto the monoblock, with two fitting pins ensuring the lateral positioning (tip/tilt/clocking), again with a ± 10 µm tolerance. Unfortunately, we found that the fitting bores in each mount plate were manufactured approximately 50 µm too wide, which is certainly the single largest alignment error in this prototype system. The baffles for preventing the stray light paths were 3D printed and painted black together with the interior of the housing. The OLED display was mounted onto a precision linear stage with a travel distance of 10 mm, ensuring a focusability from -5 to $+5$ diopters. The complete system assembly with optics, baffles, housing and eyecup is shown in Fig. 6.

We used various test patterns and full HD (1920×1080 pix) still images for visual inspection of the image quality. The naked eye with and without diopter correction could not detect any loss of image quality compared to looking directly onto a large full HD display with no optics in between, except for a small, acceptable level of distortion. The images looked perfectly sharp across the complete FOV, with high contrast and no variation of color across the field. In other words, all remaining aberrations were too small to be detected by the human eye of an observer. Except for distortion, test viewers had the impression of "looking through a hole in the wall onto a large LCD TV display", with no optics in between. Franz Kraus, a longtime CTO at ARRI, testified that the viewfinder image is "about the best I've ever seen, in terms of exit pupil,

Optics EXPRESS

Fig. 5. Stainless steel monoblock housing cut using electrical discharge machining.

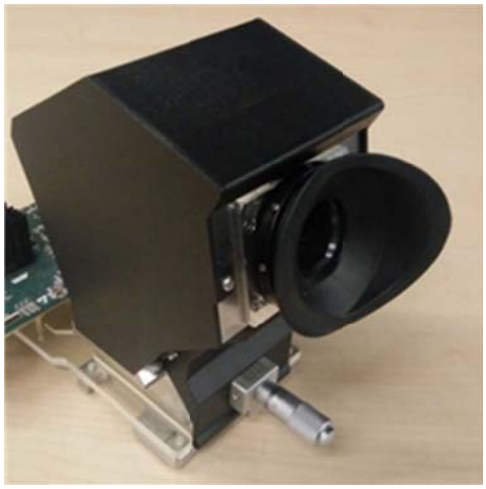

Fig. 6. Viewfinder assembly with housing, linear stage for display positioning, and eyecup.

resolution across the field, and contrast." Also, loss of contrast was barely noticeable, despite the surface quality problems shown in Fig. 4. Thus, despite the bore hole problem described above and the less than perfect surface quality of some of the mirrors, the visual impression shows that the design is not overly sensitive to tolerances.

We also investigated the image quality beyond what the eye can resolve. We set the diopter correction to + 5 diopters creating a real, magnified image of the microdisplay in free space approximately 200 mm from the eyebox plane where a 4 mm aperture is placed to simulate the eye pupil. In a dark room, we placed a CMOS camera sensor with a much higher pixel count than the 1920×1080 resolution of the viewfinder at the magnified real image location and recorded images of a test pattern, shown in Fig. 7, that had sub patterns at five locations (center, and all four corners). The results are shown in Fig. 8. Individual microdisplay subpixels (~4 μm) are clearly visible in each sub pattern. The lower-right and upper-left show more blurring than the other locations, but the subpixels are still resolved. The fact that the aberrations are not left-right symmetric per the system design, indicates that the blurring is likely due to a misalignment(s) of the mirrors caused by the aforementioned bore hole diameter issue. To test if the asymmetry was caused by the 4 mm aperture being offset from the center of the FOV, the same test was performed without the 4 mm aperture and the same asymmetry was noted. The apparent tilt of the sub-patterns images in Fig. 8 are the result of imperfect alignment of the camera sensor that

Optics EXPRESS

captured the images to the viewfinder combined with the 2% distortion intrinsic to the system design.

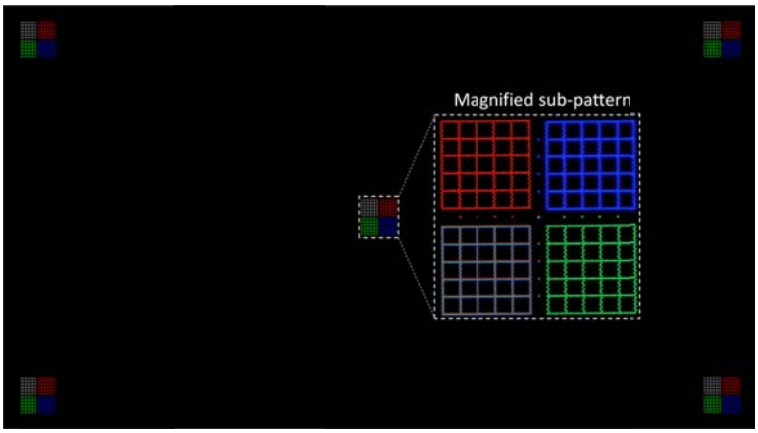

Fig. 7. The HD (1920 × 1080 pix) test pattern to be projected through the viewfinder. The center sub-pattern is shown zoomed-in as an inset. Each grid consists of single rows/columns of sub-pixels for each color. Each sub-pattern measures 730 µm on each side on the microdisplay.

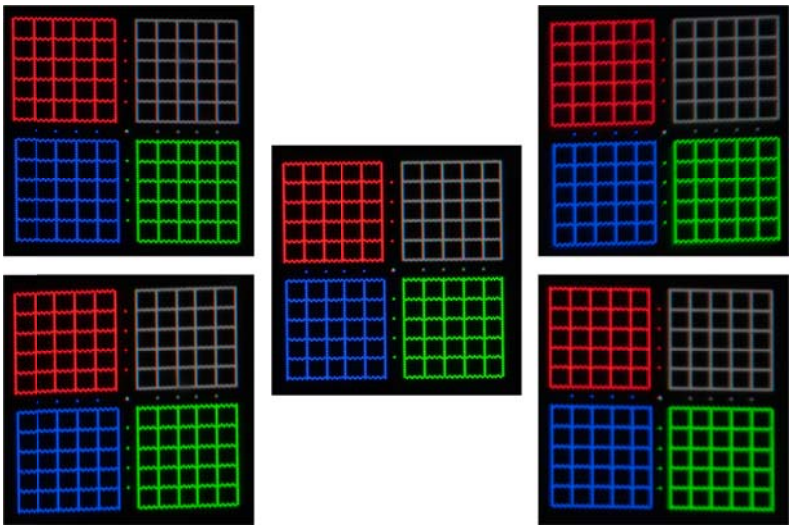

Fig. 8. Images of the test pattern displayed on the microdisplay captured by a camera sensor located at the real image produced by the + 5 diopter configuration of the viewfinder using a 4 mm pupil. The image at the center corresponds to the center of the FOV and the images in the corners correspond to the respective corner of the FOV. Each magnified sub-pattern measures 16.25 mm on each side.

5. Conclusion

We have reported results from the optical design and prototype assembly of a freeform, all-reflective professional video camera electronic viewfinder. The design uses five freeform mirrors in a compact assembly. The paths for stray light from the microdisplay to the eyebox

Optics EXPRESS

were identified and eliminated using 3D-printed baffling. The tolerance analysis predicted a manufacturable system that was then built and exceeds the strict performance requirements, giving subpixel resolution with a state-of-the-art full HD OLED microdisplay. By using only reflective surfaces, the system is completely chromatic aberration free. A correction of ± 5 diopters is demonstrated with no visible change of image quality, and an even larger diopter correction range is expected to be easily achievable with further linear movement of the microdisplay.

Funding

National Science Foundation (IIP-1338877, IIP-1338898); Arnold & Richter Cine Technik GmbH & Co Betriebs KG.

Disclosures

The authors declare that there are no conflicts of interest related to this article.

References

1. W. J. Smith, *Modern Lens Design*, 2nd ed. (Mcgraw-hill, 2004).
2. K. P. Thompson, "Description of the third-order optical aberrations of near-circular pupil optical systems without symmetry," J. Opt. Soc. Am. A **22**(7), 1389–1401 (2005).
3. J. M. Sasián, "How to approach the design of a bilateral symmetric optical system," Opt. Eng. **33**(6), 2045–2061 (1994).
4. K. Fuerschbach, J. P. Rolland, and K. P. Thompson, "Theory of aberration fields for general optical systems with freeform surfaces," Opt. Express **22**(22), 26585–26606 (2014).
5. A. Bauer and J. P. Rolland, "Design of a freeform electronic viewfinder coupled to aberration fields of freeform optics," Opt. Express **23**(22), 28141–28153 (2015).
6. A. Bauer, E. M. Schiesser, and J. P. Rolland, "Starting geometry creation and design method for freeform optics," Nat. Commun. **9**(1), 1756 (2018).
7. L. G. Cook, "Three mirror anastigmatic optical system," US Pat. No. 4,265,510 (1981).
8. S. Kim, S. Chang, S. Pak, K. J. Lee, B. Jeong, G-j. Lee, G. H. Kim, S. K. Shin, and S. M. Yoo, "Fabrication of electroless nickel plated aluminum freeform mirror for an infrared off-axis telescope," Appl. Opt. **54**(34), 10137–10144 (2015).
9. K. Fuerschbach, K. P. Thompson, and J. P. Rolland, "Interferometric measurement of a concave, phi-polynomial, Zernike mirror," Opt. Lett. **39**(1), 18–21 (2014).
10. K. Fuerschbach, G. E. Davis, K. P. Thompson, and J. P. Rolland, "Assembly of a freeform off-axis optical system employing three phi-polynomial Zernike mirrors," Opt. Lett. **39**(10), 2896–2899 (2014).